

Lifetime-based Optimization for Simulating Quantum Circuits on a New Sunway Supercomputer

Yaojian Chen
Tsinghua University
Beijing, China

Yong Liu
National Supercomputing Center in
Wuxi
Zhejiang Lab, Hangzhou, China

Xinmin Shi
Information Engineering University
Zhengzhou, China

Jiawei Song
National Supercomputing Center in
Wuxi, China

Xin Liu
National Supercomputing Center in
Wuxi
Zhejiang Lab, Hangzhou, China

Lin Gan
Tsinghua University
National Supercomputing Center in
Wuxi, China

Chu Guo
Information Engineering University
Zhengzhou, China

Haohuan Fu
Tsinghua University
National Supercomputing Center in
Wuxi, China

Jie Gao
National Research Centre of Parallel
Engineering and Technology
Beijing, China

Dexun Chen
National Supercomputing Center in
Wuxi, China

Guangwen Yang
Tsinghua University
National Supercomputing Center in
Wuxi
Zhejiang Lab, Hangzhou, China

Abstract

High-performance classical simulator for quantum circuits, in particular the tensor network contraction algorithm, has become an important tool for the validation of noisy quantum computing. In order to address the memory limitations, the slicing technique is used to reduce the tensor dimensions, but it could also lead to additional computation overhead that greatly slows down the overall performance. This paper proposes novel lifetime-based methods to reduce the slicing overhead and improve the computing efficiency, including, an interpretation method to deal with slicing overhead, an inplace slicing strategy to find the smallest slicing set and an adaptive tensor network contraction path refiner customized for Sunway architecture. Experiments show that in most cases the slicing overhead with our inplace slicing strategy would be less than the Cotengra, which is the most used graph path optimization software at present. Finally, the resulting simulation time is reduced to 89.1s for the Sycamore quantum processor RQC, with a sustainable single-precision performance of 308.6Pflops using over 41M cores to generate 1M correlated samples, which is more than 5 times performance improvement compared to 60.4 Pflops in 2021 Gordon Bell Prize work.

Keywords: quantum computing, circuit simulator tensor network contraction, Sunway architecture, slicing, direct memory access, fused design

1 Introduction

Quantum computer has the potential to provide exponential speedups over classical counterparts in specific tasks. The declaration “Quantum Advantage” refers to those tasks that can only be solved in reasonable time by using quantum computers[1][2][3]. However, despite such advantages in the computing capability, low fidelity is still the major challenge for quantum computers [4]. Classical simulators are therefore important to provide validations for quantum computer design [5]. Furthermore, scientists and researchers in areas that heavily rely on reliable computing resources, such as quantum algorithm, quantum programming language, and quantum compiler, can work on classical simulators and obtain close performance[6]. Considering both the exponential complexity and the urgent demand, improving the efficiency of the state-of-the-art classical simulator is important.

Directly storing an arbitrary quantum state on a classical computer requires an exponential amount of memory against the number of qubits. So the brute-force method to simulate quantum circuits is currently limited to less than 50 qubits[7]. In recent years the tensor network contraction (TNC)[8] algorithm has demonstrated promising potential, especially in simulating random quantum circuits (RQCs). When combined with the slicing technique, the TNC algorithm could efficiently simulate larger quantum circuits using only a limited amount of memory.

In TNC algorithm, qubits and quantum gates are represented as tensors, and the whole quantum circuit is treated as

a tensor network [9]. The problem of computing amplitudes of the output quantum state is transformed into contracting the corresponding tensor networks. The performance of TNC is mainly determined by the TNC path. In a network with hundreds of tensors, a good contraction path can easily reduce the complexity by several magnitudes compared to the bad ones. In the meantime, during the contraction process, huge intermediate tensors could appear. The slicing technique can reduce the memory requirement[10] [11], at the price of some computational overheads. This work aims to reduce the computational overhead caused by slicing.

Unlike previous efforts that predominantly use heuristic algorithms, this work introduces a new conception, *lifetime*, in order to provide better interpretability for the slicing optimization in tensor network contraction. *Lifetime* describes how an edge affects the TNC process by analyzing all the tensors and contractions it is involved in. By using *lifetime*, one is able to transform the computation into an equivalent form with much less memory requirement. Slicing works on each two adjacent manually controllable levels on a multi-level storage system. For Sunway architecture (a most advanced supercomputing system in China), both the data exchange from hard disk to main memory, and from main memory to local data memory (LDM) (*i.e.* process level and thread level), can be optimized by slicing. For process level, we slice tensors for distributed storage and parallelization, and apply *lifetime*-based slice finder to reduce the overhead of process division. For thread level, slicing helps design a fused algorithm to reduce memory access, and transform the memory-intensive kernels into computationally intensive ones in some cases, thus improving the optimization capability.

Major contributions of this work include:

- A conception, *lifetime* of graph edges (tensor dimensions), is proposed to explain the influence of each dimension, how slicing eliminates this influence, what is the origin of the slicing overhead, and how to avoid this overhead.
- Guided by *lifetime*, a dynamic slicing method with a new target function is proposed, to help find smaller slicing set with less slicing overhead.
- Indicated by *lifetime*, a high performance algorithm for TNC that fits well with the Sunway architecture is presented.

the resulting simulation time is reduced to 89.1s for the Sycamore quantum processor RQC, with a sustainable single-precision performance of 308.6Pflops using over 41M cores to simulate generate 1M correlated samples, which is more than 5 times performance improvement compare to 60.4 Pflops in 2021 Gordon Bell Prize work.

2 Background

2.1 Tensor Network Contraction and Slicing

2.1.1 Notation. A tensor network can be treated as an undirected graph, when tensors and dimensions are denoted by vertices and edges, respectively. We define the notation similar with the work of Cotengra[12]:

We denote a graph by $G = (V, E)$. V is the vertex set, and $E \subset \{(u, v) : u, v \in V\}$ is the edge set. A map $w : E \rightarrow R$ denotes the edge weight, as well as the size on each dimension. The incidence set s_v is defined as $s_v = \{e : e \in E, v \in e\}$, for vertices set $s_V = \{e : e \in E, e \cap V \neq \emptyset\}$. Vertex contraction, which merges two vertex to one by removing shared edge and keeping the rest, can be represented as a map: $Cont : P \rightarrow V_P$, where V_P is the image set that contains all the elements of V . The new vertex after contraction, $P = \{(u, v) : u \in V_P, v \in V_P\}$ is the set of pair of vertices. $Cont(u, v)$ is a new vertex under the rules of $s_{Cont(u, v)} = \{e : e \in (s_u \cup s_v - s_u \cap s_v)\}$. Based on these definitions, tensor network contractions can be represented as vertex contractions.

If we perform the pairwise contraction sequentially till there's only one vertex left, the contraction order would form a contraction path. Obviously some subsets of the contraction whose preimage set have empty intersection are independent from each other. So the contraction path are not a decisive expression. All equivalent paths can be uniquely described by a tree structure. A contraction tree B is defined as $B = (N_B, E_B)$, with each edge denoted by a vertex of original graph or an intermediate vertex generated by contraction. Specially, the edges connecting to leaf nodes are denoted by vertices in V . Nodes expressed as triplet $node = (e_1, e_2, e_3)$ refer to contractions. In particular, leaf nodes such as $(1, e_1, e_1)$ can be treated as a multiplication with a scalar 1. Then leaf nodes can represent the reading process. A certain contraction path determines the direction of each contraction. By adding the final contraction as the root, as shown in Fig 1, a rooted binary tree is acquired.

As for a given contraction tree, the time and space complexity of the corresponding contracting process can be quantitatively evaluated. Specifically in the tensor network from quantum simulation, all edges have the same weight of 2. Then the space cost is just the biggest tensor existed in the contraction tree, *i.e.* $2^{\max_{e \in E_B} |s_e|}$. And the time complexity :

$$C(B) = \sum_{node \in N_B} 2^{|s_{node}|} \quad (1)$$

To minimize the memory and time cost, the two expressions above are usually treated as the target function.

For large tensor network, memory limitation is always a serious issue. So after a path is found, it is necessary to decide whether slicing is needed to reduce the dimension of tensors. Slicing a tensor alongside a dimension (shortening as slicing a dimension in the following) can transform an

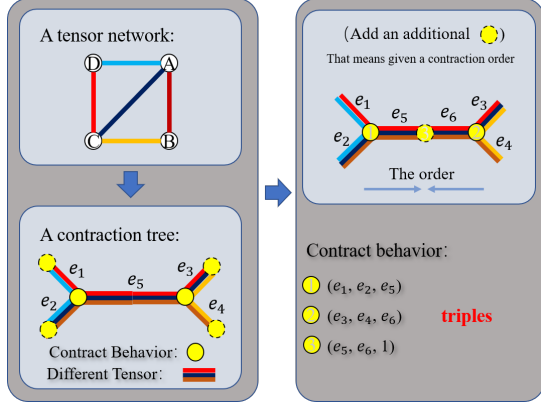


Figure 1. Tensor network and its contraction tree. When a certain contraction path is formed, an additional contraction for the final scalar should be added.

n -dimension tensor into w different $(n - 1)$ -dimension tensors. Fig 2 shows a simple example of slicing. Each of the w produced tensor involves an embarrassed parallel task. As a result, s sliced dimensions needs 2^s independent tasks, and the result will be accumulated after their individual calculation. Total time complexity may increase after slicing under some circumstance, then slicing overhead is defined as:

$$O(B, S) = \frac{C_{slice}(B) \times 2^{|S|}}{C_{original}(B)} \quad (2)$$

where s denotes the number of sliced dimensions. Slicing overhead comes from redundant calculations which can hardly be stored and reused. At a higher perspective, slicing provides a distributed storage strategy, since large tensors are sliced to stored and calculated in multi-processes respectively. Compared to traditional methods based on heavy communication, slicing shows its advantage by embarrassed parallel subtasks. However, as the price, slicing overhead determines the effect, so the major target of this work is to explain and reduce such overhead.

2.1.2 Related Work. The demand for slicing originates from the considerable memory cost of high-dimensional tensors. In some quantum advantage circuits, there are tensors with dimensions of more than 60[12]. They can occupy up to 1000 PB, which exceeds most storage systems. Slicing helps reduce the memory demand to the level of TBs or even GBs to make simulation feasible.

Cotengra[12] integrates several anytime methods and claims over 10000 \times speedup compared to the estimation made by Google[1]. It introduced some effective heuristic algorithm for contraction path searching, such as community[13] and graph partition[14]. After the pre-process which is implemented in [15], rank-1 and rank-2 tensors are absorbed, and the tensor network is largely simplified. A greedy-based slicing strategy is built in cotengra. It repeatedly chooses a dimension that leads to the most minor overhead to slice,

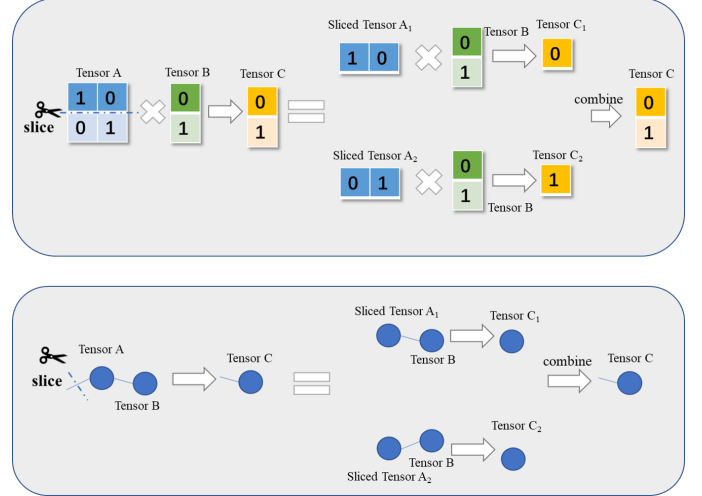


Figure 2. An intuitive example of slicing. The second half expresses with graph as a parallel.

until the memory demand is satisfied. Like most greedy methods, local minimum exists in this slicing strategy. In our work, cotengra is applied to find a proper contraction path.

Alibaba proposed a simulator based on an observed structure called 'stem'[16]. A stem is a computationally-intensive region in the contraction tree, including most high-dimensional tensors. The inexpensive parts are called branches. Within a single stem, a bigger tensor sequentially absorbs smaller ones, and about 99.99% computation cost happens during these contractions. The slicing strategy is a dynamic process. While basic logic is the same as Cotengra, they perform local tuning of contraction tree between two steps of slicing picking. This dynamic design highly reduced the inherent slicing overhead of a contraction tree. However, given a certain path, this strategy may not be able to find an optimal slicing set. Recently, cotengra has updated this strategy as "slicing reconfigure", too. This work can provide $10^{18.8}$ times complexity, slicing overhead of 4, and a 14.7% FLOPS efficiency.

As for the New Sunway System, several efforts study high-performance algorithms for TNC. Customized for new architecture, Sw_Qsim[17] provides a series of methods for matrix multiplication and tensor permutation, especially for narrow tensors. The work that won the 2021 ACM Gordon Bell prize[6] implemented Transpose Transpose GEMM Transpose (TTGT) algorithm on Sunway architecture, which is a fused design of tensor permutation and matrix multiplication in order to reduce memory access. These efforts significantly improve the FLOPS efficiency, but all concentrate on one step of the whole path instead of taking a holistic view. Optimization will soon reach the ceiling as a bandwidth-constrained problem according to Roofline model.

2.2 New Sunway Supercomputer

As a heavy time- and memory-consuming part, performing the actual contraction generally requires support from sophisticated supercomputers. A new Sunway supercomputer is selected for this work.

The new-generation Sunway supercomputer has a similar architecture as Sunway TaihuLight[18], with the major computing capability provided by core groups (CGs). A heterogeneous many-core processor, SW26010pro, is designed for this supercomputer. Fig 3 shows the structure of the chip. Each processor chip has 6 CGs. The computing processing elements (CPEs) of each CG are arranged as an 8 by 8 grid. A loop network-on-chip (NoC) connects the CGs and undertakes the task of communication.

Each CG contains a 16GB main memory, and each CPE contains 256KB local data memory (LDM). Direct memory access (DMA) with a bandwidth of 51.2 GB/s is provided between LDM and main memory. Due to the enormous arithmetic intensity, the memory access bottleneck often turns to the vital problem for optimization. Remote memory access (RMA) with a peak bandwidth of more than 800 GB/s is designed for data exchange between CPEs within one CG. RMA provides similar function-like communication without waiting, and results in a entirely different computation-communication overlapping alternative compared with the previous-version TaihuLight [18] system.

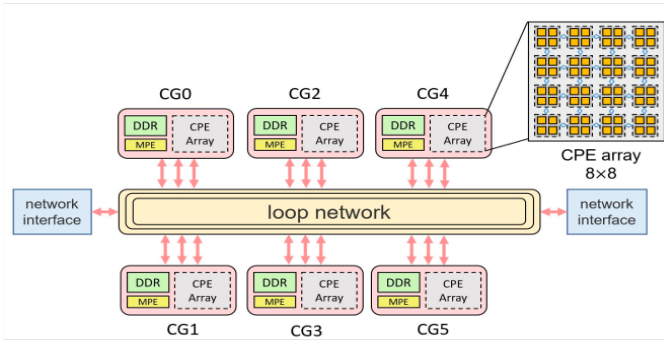


Figure 3. SW26010pro Processor[17]

3 Lifetime

For brevity, please refer to the supplementary material for part of the lemma and proof.

3.1 Definition

Here is a simple example showing where the slice overhead comes from. Fig 4 shows a contraction process on a 4×2 tensor network. If we apply a contraction path and slice tensors as shown in the figure, the two sliced tensors drop one dimension, respectively. Analyzing the time complexity in Fig 4 before and after the slicing, the steps affected by slicing form a linear area, and only in this area the total time

complexity is held. Since the tensors outside have nothing to do with the sliced dimension, their correlated calculations will be doubled.

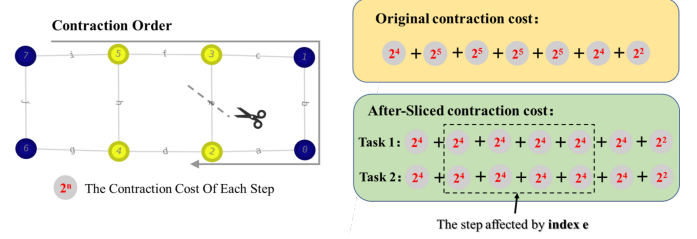


Figure 4. A sample to show the origin of slicing overhead. The sliced dimension only exists on two tensors in the original TN, and its sphere of influence is just the area between these two tensors. As the right shows, only the steps on a line inside the dashed box keep their time complexity.

Based on the analysis above, this work proposed a new concept, *lifetime*, to describe the scope of influence of a sliced dimension during the slicing. The notation comes from section 2.1.1.

Definition 1. Given a tensor network $G = (V, E)$ and a contraction tree $B = (N_B, E_B)$, the concept *lifetime* of a edge index $k \in E$ refers to a set of tensors $\{T_{i_1}, T_{i_2}, \dots, T_{i_n}\} \subset E_B$, if $k \in s_{T_{i_j}}$, for all $1 \leq j \leq n$.

With the definition of *lifetime*, the scope of influence of a sliced edge is clearly represented. We can conclude that, after slicing an edge e from a tensor network, the size of tensors on the lifetime of e will be halved while the size of the others will not change. The time complexity of the contractions corresponding to these tensors will not be changed, while the time complexity of the other contractions will be doubled.

Not merely on the whole contraction tree, *lifetime* can be conveniently defined recursively on each of the sub-tree or intermediately generated tree during the contraction process by simply replacing the contraction tree in the definition. The advantage here is that we can focus more on the region with intensive computation. Recent work led by Alibaba[16] presented an observed structure, stem from Sycamore circuit[1], which is defined as a path formed by high-weights tensors. After pre-calculating every branch, stem can be treated as a highly unbalanced contraction tree, and we are able to define *lifetime* on it.

3.2 The Origin of Slicing Overhead

Large tensor networks from big circuits such as Sycamore and $10 \times 10 \times 40$ RQC often needs to slice dozens of edges, which makes multi-edges slicing a central problem for complexity analysis. Considering that *lifetimes* of different edges

are independent, slicing an edge of index a has nothing to do with the *lifetime* of index b . So each sliced index can be analyzed one by one. Fig 5 provides an example of the slicing of two indices, and shows that the overall overhead of each contraction is the production of all sliced edges. Expanding to a general circumstance, if a tensor contains s sliced indices with totally n , it will be divided into 2^s smaller tensors. For all 2^n subtasks, there will be 2^{n-s} times of redundant data. Similarly, for correlated contractions with s sliced indices involving calculation, the time complexity will be multiplied by 2^{n-s} times. As a result, the density of *lifetimes* plays a decisive role in memory and computation complexity in a region.

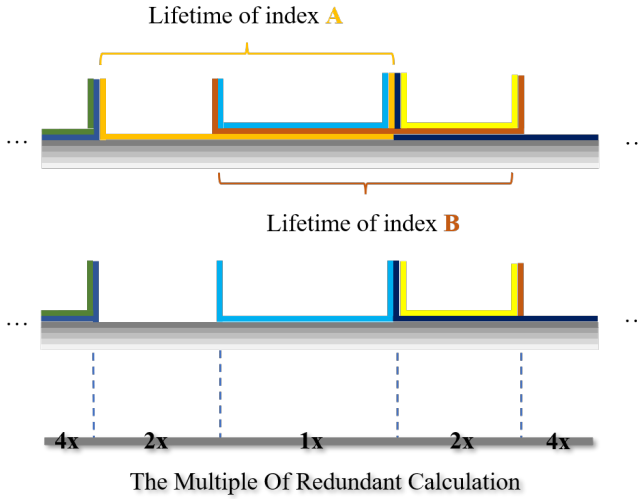


Figure 5. Overlap of lifetime. From the left to the right, the contraction tree is divided into 5 parts, lifetime of index A goes through part 2 and 3, while B goes through part 3 and 4. Index A and B double the time complexity of part 1, 4, 5 and part 1, 2, 5 respectively, and make the whole multiple of redundant calculation showed above as a production.

The number of sliced edges is another essential variable. More slicing has to be performed if the memory demand is not appropriately satisfied. For a practical path from the common quantum advantage circuits, tensors on the path only carry dozens of edges. Otherwise, both time and space complexity will be unacceptable. Compared to thousands of edges on the whole, there are very few edges whose *lifetimes* are across the whole contraction tree, especially for a non-linear tree. As a result, more sliced edges bring huge risks of overhead. Considering that the whole overhead is multiplied by the overhead from each sliced edge, it will grow exponentially with the number of sliced edges.

Furthermore, we can prove the theorem below. It provides interpretation for redundant slicing more profoundly, and

casts the theoretical cornerstone for our slicing strategy. It shows that, a valid smaller slicing set indicates a lower slicing overhead in most conditions.

Theorem 1. For a tensor network $G(V, E)$, a contraction tree $B(V_B, E_B)$ and a n -edge slicing set S_1 , if a $(n - 1)$ -edge slicing set S_2 is found, and the intersection of S_1 and S_2 is not empty, then there must exist an $(n - 1)$ -edge slicing set S_3 , whose overhead is less than S_1 .

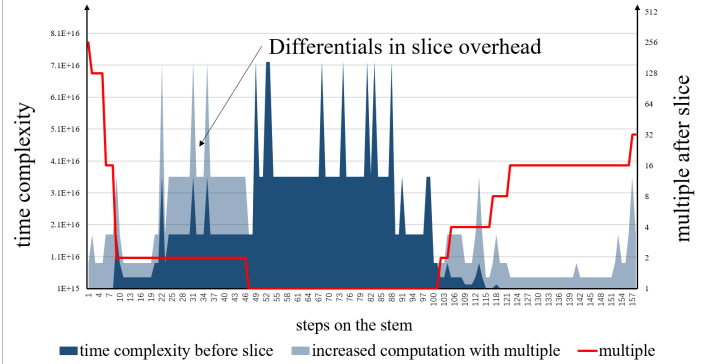


Figure 6. Time complexity and multiple by slicing on stem (Sycamore($m = 20$) is used as an example).

Fig 6 compares the whole time complexity before and after slicing on a common contraction tree of quantum advantage circuits. From the figure, we can conclude that the key to a low overhead is that the time complexity of the main computation-intensive part is kept, which means big tensors are contained in lifetimes of as many as sliced edges. Ideally, time complexity and the slicing caused multiple are negatively correlated.

3.3 Route of Slicing Optimization

According to the discussion above, the relationship between the number of sliced edges and slicing overhead is by degrees clear. Due to the memory bound, we have to do the slicing, and the overhead reduction becomes a major work. However, on a multi-level storage system, different strategies should be applied to avoid slicing overhead for different levels.

For TNC, we have summarized that there are two main methods to deal with the overhead, *i.e.*, to stack or to reduce overhead by searching for better slicing sets. Stacking is the inverse operation of slicing, and is feasible when the capacity of the low level of storage or distributed memory is enough for the whole memory requirement. For example, we can store the rank-53 tensor in the hard disk, get a rank-30 slice at a contraction step by IO, and then put it back after calculation. This process performs slicing by getting and stacking by putting naturally. If stacking immediately after the *lifetime* of a sliced edge ended, the overhead of this edge

is naturally eliminated, and the memory demand is resolved. Nevertheless, there will be vast costs of data exchange during data access (use low-level storage) or communication (for distributed memory). Searching for a better slicing set can avoid memory access and communication, but it introduces overhead from the redundant calculation. The choice depends on the specific value of bandwidth and overhead. In case of low bandwidth and low overhead, slicing optimization has better performance, while in case of high bandwidth and high overhead, stacking is more suitable.

Fig 8 shows a typical overhead distribution for different target sizes. The arithmetic intensities (AI) of different levels represents the equal overhead by data access. The line of AI and the storage capacities divide the graph into several parts. The commonest manually controllable storage levels include hard disk, main memory and LDM (for sunway architecture). For memory access, $BandWidth_{IO} \ll BandWidth_{DMA} \ll BandWidth_{accessLDM}$. Then, from hard disk to LDM, stacking becomes more potential, and in contrast, slicing optimization should be applied.

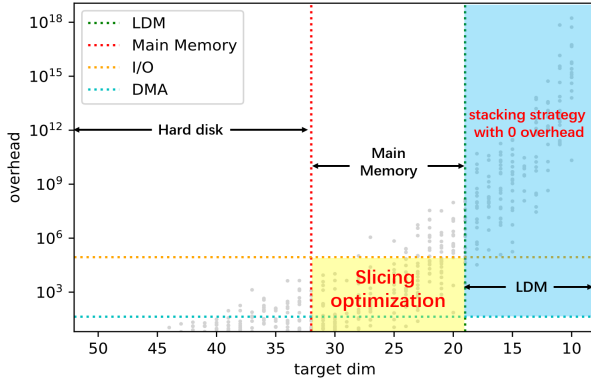


Figure 7. Overhead distribution for different storage level by cotengra. (Sycamore($m = 20$) as an example with original memory cost approximately dozens of PBs. For Sunway architecture, there is a 96GB main memory on a chip and a 256KB LDM for each CPE)

4 Slicing Overhead Reduction

4.1 Overview of Slicing Optimization

The Low bandwidth of IO restricts stacking, and the slicing overhead directly influences the parallel scalability. As shown in theorem 1, optimization of slicing can be divided into two steps: searching for a smaller slicing set, and tuning the selected slicing set to achieve a lower overhead. The following two subsections discuss these two steps separately.

Minimizing the overhead while fitting the memory bound describes an optimization problem with constraints. Given a contraction tree $B = (N_B, E_B)$, the target function can be

described by the total time complexity after slicing.

$$C(B, S) = \sum_{V \in N_B} 2^{|s_V| + |S| - |S \cap s_V|} \quad (3)$$

where S is the set of sliced edges. For the stem, the target function combines the multiply curve and the time complexity curve. Large value of $|s_V|$ represents a computation intensive region. To minimize $C(B, S)$, the two curves shall be aligned in a sense.

The target size which does not exceed the memory capacity is denoted as t . For every $e \in E_B$, $|S \cap s_e| \geq |s_e| - t$. The target function and the formula together can determine the optimization problem.

4.2 Slicing Strategy

Here we define *lifetime* on the stem. Since branches have nothing to do with the memory constraints, they are pre-contracted. Only stems remain for optimization. If there are more than one stem, we choose the most computational intensive one to start with.

Assuming the optimal size of the slicing set is s , the stem is then separated into two continuous parts: $M = M_1 + M_2$, and let the optimal size of M_1 be s_1 . For M_1 , there is a number of candidate sets that share the same size s_1 . According to the discussion above, the more tensors *lifetimes* of s_1 pass through M_2 , the less edges shall be sliced in the updated M_2 .

For slicing, an important lemma is that: longer *lifetime* does not necessarily lead to lower slicing overhead. But the containment relationship of *lifetime* does. So is the effect of reducing memory. In particular, for the leaf nodes of the contraction tree, there is only one extension direction, then its length decides the containment relationship. So we start the search from the two ends of the stem, and choose one tensor as M_1 each time and the left part as M_2 . Therefore, an edge with longer *lifetime* shall be better. If we perform this process iteratively, a smaller slicing set is expected. We propose Algorithm1 for details.

Though the above strategy does not always provide the slicing set with the lowest overhead, sometimes even worse than the one found by cotengra, we have successfully satisfied all the prerequisites of the theorem above. The method above can find a slicing set as small as possible for a given contraction tree. Combined with the dynamic process for path searching, the overhead may drop lower. As a result, a better slicing set will be found by the refiner to reduce the overhead.

4.3 Slice Refiner based on Simulated Annealing

Our slice finder can not guarantee finding an optimal slicing set, and it looks for one as small as possible. So, the main task of this section is to find the best one given a certain number of sliced edges. Considering that the number of edges of the set we found and the target slicing set is the same, the

Algorithm 1 Procedure slice finder

Input: Stem of contraction tree M , target dim t
 $N = \text{len}(M), S \leftarrow \emptyset, lf = \text{dict}()$
for all edge indices in M **do**
 Calculate $lf[\text{index}]$
end for
repeat
 $sT = (M[0].\text{dim} < M[N-1].\text{dim}) ? M[0] : M[N-1]$
 Add $sT.\text{dim} - t$ indices with longest lifetime into S
 for all $T \in M$ **do**
 if $T.\text{dim} \leq t$ **then**
 $M.\text{remove}(T)$
 end if
 end for
 Update lf, N
until $N == 0$
Output: slicing set S

permutation from the former to the latter can be described as edge replacement.

After slicing, there are some tensors whose dimensions are exactly equal to the target dimension, and they are named "critical tensors". If the lifetime of a sliced edge contains none of the critical tensors, this edge does not contribute to memory reduction, and can be removed from the slicing set. Moreover, in another angle of view, to replace a sliced edge with index a , a direct way is to find another unsliced index b whose lifetime contains all critical tensors in the lifetime of a .

Simply replacing indices one by one sometimes leads to a local minimum. For instance, the optimal set contains index a and index b while the one we found contains c and d , but replacing c from a may increase the overhead, or fail to match the memory bound. Under these circumstances, the strategy should endure a temporary complexity increase, then simulated annealing helps.

For one index, there are several candidates being able to replace it based on critical tensors. For more indices, we start from 2 indices, and call slice finder to find the candidates for the replacement, until there is no proper candidate found. Then, our strategy chooses the best one among the candidates and accept it by possibility. After refinement, the overhead can be further reduced.

5 Fused Design Based on Secondary Slicing

5.1 Difficult for Thread Level Optimization

For thread level, if organizing the whole path on the CPEs, considering the 256-KB LDM, there will be a huge overhead. As a result, previous works optimize on thread-level step by step[17][6] to avoid it, turning to memory access instead of vast redundant calculation. However, frequent memory access also limits the FLOPs efficiency a lot.

Contraction between tensors is implemented by matrix multiplication[17]. Based on this strategy, near-optimal FLOPS can be obtained on square-like matrices. However, For narrow matrix multiplication, especially 2 of m, n, k is less than 16, which is dominant in many simulation tasks[1], we can see $\Theta(MNK) \approx \Theta(MN + NK + MK)$, and GEMM will change from a computational intensity problem to a bandwidth-constrained problem. Another limitation comes from the 256-KB LDM on each CPE, which can only hold a rank-13 tensor for multiplication. Then, calculating a contraction by a rank-31 tensor at least needs 2^{12} times for a CG.

To take full advantage of the 512-bits single instruction multi-data (SIMD), a 4×4 complex GEMM kernel is applied. But in the cases when k, n are both small, for instance, 2, 3, 4, ..., the demand of data length will cause a conflict between the high-performance kernel and the 2D data distribution. In contrast, 1D distribution avoids most padding, and slices the GEMM process into simply paralleled subtasks. Most importantly, the implicit slicing embedded in data distribution, as a method to overcome the memory limitation of LDM, has a similar problem with slicing on the process level.

We propose a more efficient slicing and stacking strategy called **secondary slicing** on thread level, and can heavily reduce the cost of DMA. Secondary slicing between LDM and the main memory, which will provide a fused operator to organize parts of contraction path on CPEs, and greatly save the time of memory access.

5.2 Secondary Slice for LDM

In order to achieve an acceptable memory cost, we need to reduce the dimension of intermediately generated tensors. If the memory requirement is not satisfied, we will be forced to use the hard disks for storage. Fortunately, due to slicing, the colossal memory demands are divided into numbers of uncorrelated subtasks, then can be resolved by a stream-like strategy. Then, the whole contraction path can be performed on a process without intermediate communication and IO. An abstract model of this method is that, in a multi-level storage system, between two adjacent manually controllable levels, even with a huge difference in capacity, slicing points out the parallelism or the potential to apply data flow, then reduces the memory requirement for feasibility with some computation overheads.

Such a strategy is available between LDM and the main memory. Since LDM on the new Sunway supercomputer is only feasible for a rank-13 tensor, if the contraction is performed step by step, we should frequently do DMA-get and DMA-put between every two steps. Considering the arithmetic intensity above, memory access will be dominant. To reduce the frequent data exchange between LDMs and the main memory, performing n steps of the contraction path successively in one computation kernel helps. At the beginning of those steps, we do DMA-get once to get the bigger tensor, and after n steps of calculations, the result will

be written back by DMA-put. Then, $n - 1$ times of DMA-get and DMA-put are reduced.

Organizing parts of the contraction path in CPEs can be implemented similar to the one in MPEs. The primary difficulty comes from memory bound and the parallel framework. As the top half of Fig 8 shows, CPEs can obtain a lower rank tensor from the one in the main memory at each time, throwing out some dimensions. In a particular contraction, commonly, there are parts of dimensions absorbed, and the others held. According to this observation, at the beginning of the computation, if we choose all dimensions which will be absorbed in the following n steps to form a tensor, and get it into LDMs by DMA with stride, then each CPE can do the calculation independently, like the bottom half of Fig 8 shows. As for the memory bound, we tune the parameter n to determine the rank of the formed tensor.

In this strategy, the chosen indices remain, and the other indices are sliced. Different CPEs do different subtasks generated by slicing, which is embarrassingly parallel. The main question is how to choose sliced indices and find a proper n . The fundamental prerequisite for the slicing set is that the sliced indices will not be contracted in n steps, and fortunately, such a condition is just the definition of *lifetime*. So with a particular start position on the path, which is also an end of *lifetime*, we traverse the remaining stem, on which each position forms a sub-path. All indices whose *lifetime* cross the sub-path form the slicing set. If the size of slicing set added by 13 is less than each of tensor on the sub-path, the fused calculation finished. With this strategy, there's no slicing overhead, and the last DMA-put plays the role of stacking with no extra communication.

5.3 Deep Optimization

5.3.1 Permutation Map Reduction by Recursion Formula. In situ computing map and the pre-calculated map are two primary methods for the tensor permutation. The in situ computing map needs an $O(N \log N)$ time complexity for a size- N tensor with rank $O(\log N)$, and an $O(1)$ space complexity. In contrast, the pre-calculated map provides $O(N \log N)$ time complexity for the first computation and $O(N)$ for the next ones, and space complexity of $O(N)$. In our fused algorithm, permutations before every step of contractions become one of the hot spots. Even though using short type, n pre-calculated maps are too big to store. However, for strategy based on in situ map, the tensors' ranks are about 10, which leads to more than 10 times the cost.

A feasible solution is to combine the advantage of the two strategies. For a specific contraction, $A^T B^T = C$, in which T denotes permutation, a typical indices order of a rank-9 A after permutation is like 0, 1, 2, 4, 5, 7, 8, 3, 6, the indices need to be absorbed will be organized at the end, i.e., 3, 6. Contrary to A , such indices are placed at the beginning, like 3, 8, 0, 1, 2, 4, 5, 6, 7. For A , obviously, the first 3 dimensions will not participate in the permutation, so only a 1/8 map is

enough. And for B , the last 4 dimensions are the same during the permutation, so the adjacency of the 4 elements shaped by 4, 5, 6, 7 will be held, and the size of the map is reduced to 1/16. With adding an offset, map of the corresponding can be calculated by $map[i + k] = map[i] + k * offset$ when $k < stride$ in $O(1)$, the same as pre-calculated map. The space complexity will be reduced to $O(N/2^m)$, where m is the number of continuous indices at the end or beginning.

5.3.2 Optimization for Stride DMA by RMA. Though the fused strategy heavily reduces DMA, the efficiency of stride DMA becomes an obstacle. If we want to get a sub-tensor with indices 1, 3, 5, 7, 9, 11, 13, 15 from a rank-17 tensor in the main memory, one stride DMA get can hardly work. After getting the first element, the next has a stride of 1, and then a stride of 4, and so on. We need a totally 2^7 times of stride DMA-get with poor granularity to get the whole rank-8 tensor. Under this circumstance, the bandwidth of DMA-get can only achieve 32MB/s, 1000 times lower than the peak performance, and makes negative optimization.

To improve the bandwidth, cooperation of 64 CPEs becomes essential. In such a rank-17 tensor, under our parallel framework, the last 6 sliced indices are organized between 64 CPEs. Data exchange is much faster between CPEs by Remote memory access (RMA), whose peak performance can achieve near 1000GB/s for a whole CG. For the example above, let each CPE get a rank-8 tensor of 9, 10, 11, 12, 13, 14, 15, 16, and the DMA granularity is improved to 2^8 , which will fully utilize the peak bandwidth. Then, since indices 10, 12, 14, 16 are the global indices between CPEs, RMA helps to do the data exchange, transforming 10, 12, 14, 16 into 1, 3, 5, 7. To achieve a high bandwidth for RMA, we do a permutation to reshape data to 10, 12, 14, 16, 9, 11, 13, 15 to guarantee the granularity of RMA. For DMA-put, the process is similar.

6 Result

Related efforts (e.g., Cotengra[12], Alibaba[16] and [6]) have all simulated Sycamore RQC[1]. To make an appropriate comparison, unless otherwise specified, the contraction trees used in this work come from the tensor network of Sycamore as well.

6.1 Slicing Overhead and Scaling Result

According to the slice strategy in 4, given a contraction path, we can find a slicing set with lower overhead in expectation. Fig 9 shows the comparison between our work and cotengra. We find 400 contraction paths by cotengra, and apply our method and cotengra respectively to search for slicing sets. Compared with cotengra, the slicing sets we found are potentially smaller, and lead to lower overhead. Specific to each path, the {better, same, worse} triple of slicing size and overhead are {150, 240, 10} and {180, 210, 10} respectively.

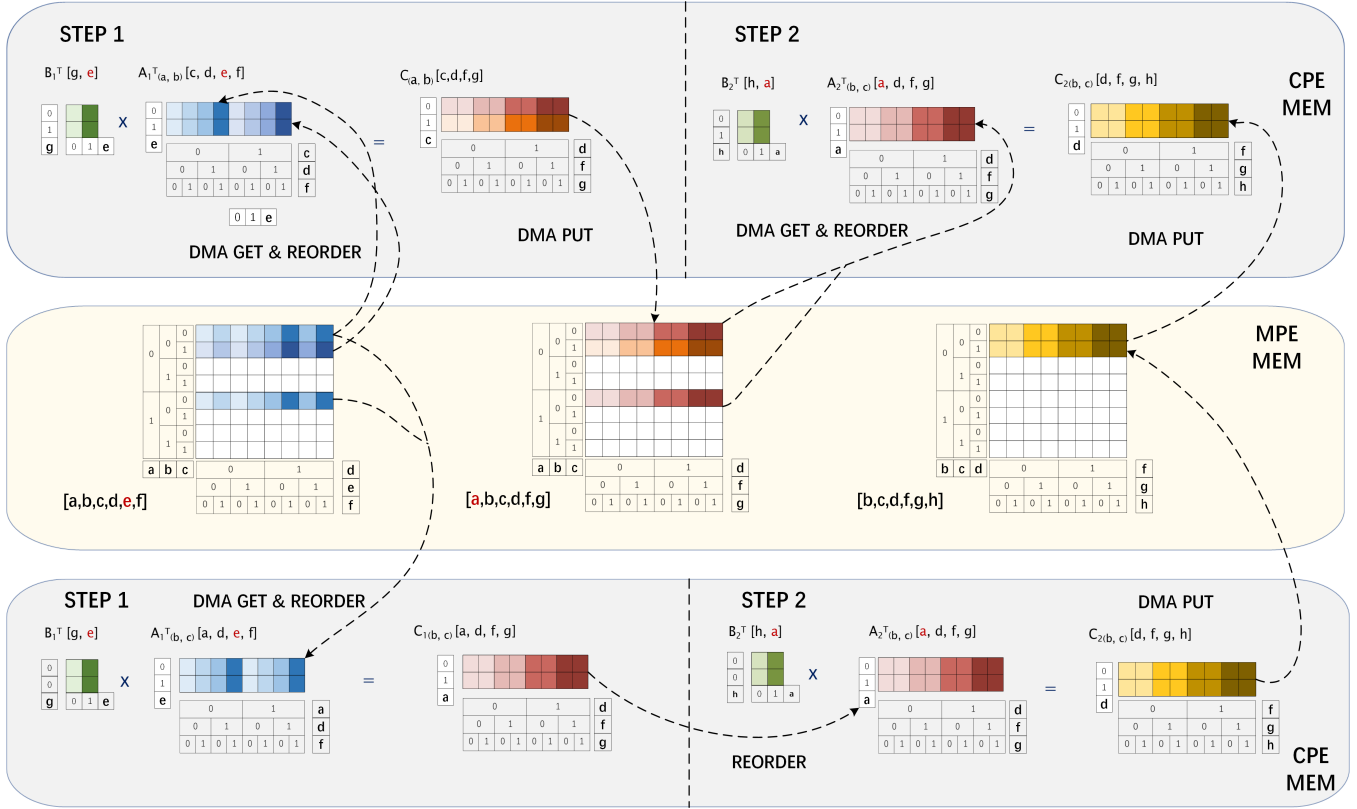


Figure 8. A fused design for thread level optimization. The top half shows the step-by-step strategy in previous work, and ours organized a sub-path on the LDM, and reduce $n - 1$ times of DMA-get and DMA-put for an length- n sub-path. The superscript T denotes permutation, and the subscript of tensors denotes the sliced dimensions.

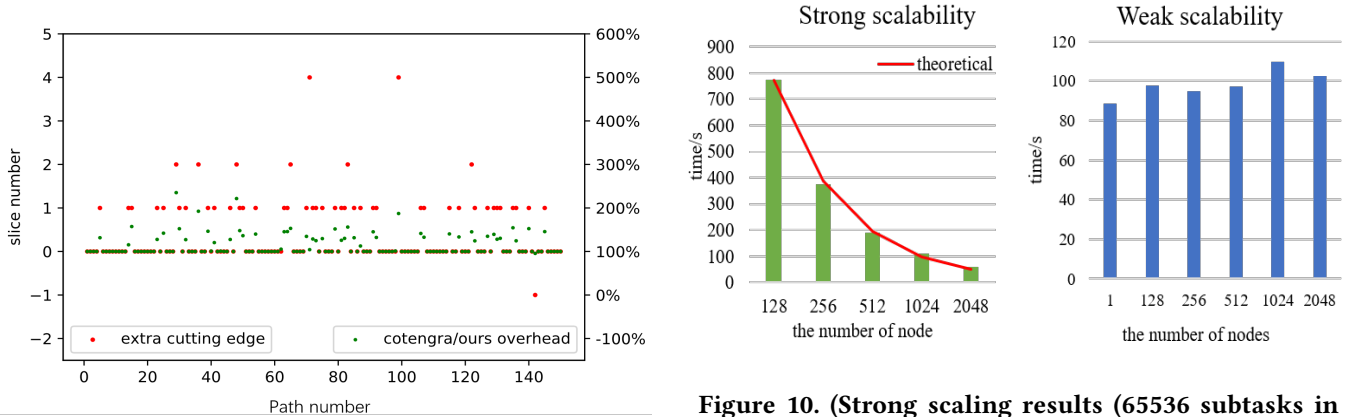


Figure 9. Slicing size and overhead compared with cotengra. The red points shows the number of extra slicing edges by cotengra compared with ours; and the green points shows the ratio of overhead. When the difference is 0 and the ratio is 100%, two method perform equally.

The best overhead result we found is less to 1.05, and we comprehensively choose a path with low complexity to do the thread level optimization.

Figure 10. (Strong scaling results (65536 subtasks in total) and weak scaling results (16 subtasks on each node)).

Due to slicing, processes are highly independent with each other, and will only do *allReduce* once at the end of program. The strong scaling results and weak scaling results are showed in Fig 10.

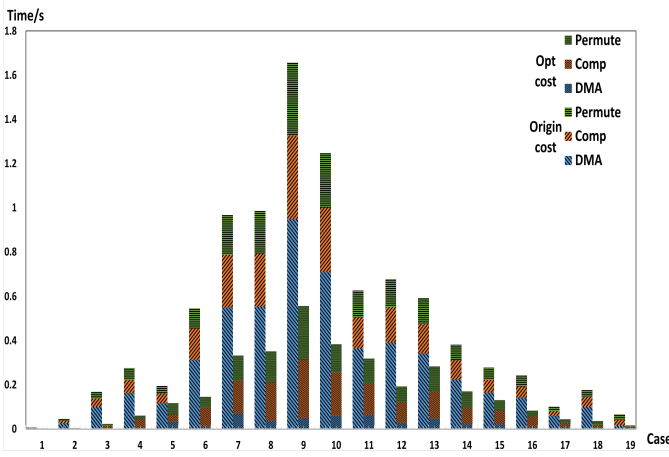


Figure 11. Optimization by secondary slicing at the thread level. Optimization is done on a single node with 390 cores, and the performance is tested for tasks with different size on a contraction path. Use the step-by-step strategy for comparison.

6.2 Computing Efficiency

Fig 11 shows that our work is able to significantly improve the computing efficiency, and reduce the time cost of a sub-task from 11.2s to 2.23s. Therefore, we project that we can reduce the whole time cost using 107520 nodes (41,932,800 cores) to 89.1s with a sustainable single-precision performance of 308.6Pflops.

According to Fig 11, the time of memory access is largely reduced by secondary slicing, and the time of permutation and GEMM keep similar. This result verifies our prediction that, secondary slicing can reduce memory access with the price of some python based pre-conditioning, which needs only 1 core and ignorable time. Another conclusion is that, after secondary slicing, the computation kernel is transformed from a memory intensive one to a computation intensive one in some cases. According to Roofline model[19] and the arithmetic intensity of Sunway architecture, the number of floating point operations should exceed 42.3 times of number of bytes of memory access to achieve a peak performance. The average fused steps of our strategy is about 10, and there is $MNK/(MN + MK + NK) \approx K$ for a small K with a average of 4, then in some cases the arithmetic intensity of TNC can break through 42.3. Fig 12 shows the Roofline model for a particular case on thread level. Due to permutation, which consists of LDM access, there is still a gap between our performance and the peak performance. However, compared with the original arithmetic intensity of 2.x, the optimization limit is largely improved.

7 Implication

In this paper, we presented novel *lifetime*-based methods to reduce the slicing overhead and improve the computing

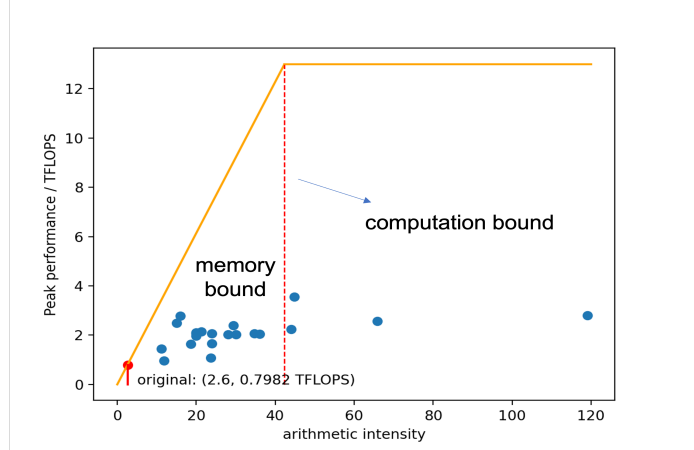


Figure 12. Roofline Model of our work. For different cases, the arithmetic intensities are different from 10x to 40x. In some cases, the problems turn into computation-bound.

efficiency for parallel optimization at both the process level and thread level.

Due to the introduction of *lifetime* definition, A series of lemmas and theorems based on *lifetime* intensify our awareness of a tensor network and the contraction trees, then an interpretable method to deal with slicing overhead, and an in place slicing strategy to find the smallest slicing set, so that we can reduce the slicing overhead less than the Cotengra[12] in most cases as shown in the experiment.

Furthermore, based on *lifetime*, we can distinguish two kinds of tensor networks which shall be sliced by different strategies, an adaptive tensor network contraction path refiner customized for Sunway architecture. That means, at the process level, we searched for a better slicing set to avoid memory access and communication, paid with little overhead from the redundant calculation. While at the thread level, we adopted stacking to avoid heavy overhead from the redundant calculation, at the necessary price of more affordable memory access by DMA and faster communication among the core-groups by RMA.

Finally, the resulting simulation time is reduced to 89.1s for the Sycamore quantum processor RQC, with a sustainable single-precision performance of 308.6Pflops using over 41M cores to generate 1M correlated samples, which is more than 5 times performance improvement compared to 60.4 Pflops in 2021 Gordon Bell Prize work. Further, if we adopt the adaptive precision Scaling method in this work, our simulation time would reduce to about 50 seconds, nearly one-sixth of the time 304s[6].

In addition, *lifetime* is also very promising in future works in finding contraction paths, analyzing time complexity, and even helping us explore tensor network structures. As a widely applied approach, tensor networks can be found in

many research fields such as statistical physics[20], data science[21], sociology[22] and so on.

This work proves that *lifetime* is essentially promising for the tensor networks which have an equal edge weight and a dominant stem. Moreover, *lifetime* can be easily generalized to tensor works with different features and helps analyze both the time- and space-complexities of the contraction. In conclusion, it is foreseeable that *lifetime* can play important roles in more fields.

Acknowledgment

We would like to thank Zhen Wang, Zhaoqi Sun, Zegang Li and Yuxuan Li for advice and discussions.

This work is partially supported by National Key R&D Program of China (2020YFB0204804, 2020YFB0204800), National Natural Science Foundation of China (Grant No. T2125006, U1839206, Project No. 62102114), Jiangsu Innovation Capacity Building Program (Project No. BM2022028) and the Key Research Project of Zhejiang Lab(No. 2021PB0AC01). The corresponding authors are Yong Liu (liuy_99@163.com), Xin Liu (lucyliu_zj@163.com), Lin Gan (lingan@tsinghua.edu.cn), Dexun Chen (adch@263.net) and Guangwen Yang (ygw@tsinghua.edu.cn).

References

- [1] F. Arute, K. Arya, R. Babbush, D. Bacon, J. C. Bardin, R. Barends, R. Biswas, S. Boixo, F. G. Brandao, D. A. Buell, *et al.*, “Quantum supremacy using a programmable superconducting processor,” *Nature*, vol. 574, no. 7779, pp. 505–510, 2019.
- [2] J. Wells, B. Bland, J. Nichols, J. Hack, F. Foertter, G. Hagen, T. Maier, M. Ashfaq, B. Messer, and S. Parete-Koon, “Announcing supercomputer summit,” 6 2016.
- [3] H.-S. Zhong, H. Wang, Y.-H. Deng, M.-C. Chen, L.-C. Peng, Y.-H. Luo, J. Qin, D. Wu, X. Ding, Y. Hu, *et al.*, “Quantum computational advantage using photons,” *Science*, vol. 370, no. 6523, pp. 1460–1463, 2020.
- [4] A. Zlokap, S. Boixo, and D. Lidar, “Boundaries of quantum supremacy via random circuit sampling,” 2020.
- [5] F. Pan and P. Zhang, “Simulating the sycamore quantum supremacy circuits,” *arXiv preprint arXiv:2103.03074*, 2021.
- [6] Y. Liu, X. Liu, F. Li, H. Fu, Y. Yang, J. Song, P. Zhao, Z. Wang, D. Peng, H. Chen, *et al.*, “Closing the” quantum supremacy” gap: achieving real-time simulation of a random quantum circuit using a new sunway supercomputer,” in *Proceedings of the International Conference for High Performance Computing, Networking, Storage and Analysis*, pp. 1–12, 2021.
- [7] K. De Raedt, K. Michielsen, H. De Raedt, B. Trieu, G. Arnold, M. Richter, T. Lippert, H. Watanabe, and N. Ito, “Massively parallel quantum computer simulator,” *Computer Physics Communications*, vol. 176, no. 2, pp. 121–136, 2007.
- [8] S. Boixo, S. V. Isakov, V. N. Smelyanskiy, and H. Neven, “Simulation of low-depth quantum circuits as complex undirected graphical models,” *arXiv preprint arXiv:1712.05384*, 2017.
- [9] J. Biamonte and V. Bergholm, “Tensor networks in a nutshell,” *arXiv preprint arXiv:1708.00006*, 2017.
- [10] B. Villalonga, D. Lyakh, S. Boixo, H. Neven, T. S. Humble, R. Biswas, E. G. Rieffel, A. Ho, and S. Mandrà, “Establishing the quantum supremacy frontier with a 281 pflop/s simulation,” *Quantum Science and Technology*, vol. 5, no. 3, p. 034003, 2020.
- [11] E. Pednault, J. A. Gunnels, G. Nannicini, L. Horesh, T. Magerlein, E. Solomonik, and R. Wisnieff, “Breaking the 49-qubit barrier in the simulation of quantum circuits,” *arXiv preprint arXiv:1710.05867*, vol. 15, 2017.
- [12] J. Gray and S. Kourtis, “Hyper-optimized tensor network contraction,” *Quantum*, vol. 5, p. 410, 2021.
- [13] M. Girvan and M. E. Newman, “Community structure in social and biological networks,” *Proceedings of the national academy of sciences*, vol. 99, no. 12, pp. 7821–7826, 2002.
- [14] Y. Akhremtsev, T. Heuer, P. Sanders, and S. Schlag, “Engineering a direct k-way hypergraph partitioning algorithm,” in *2017 Proceedings of the Nineteenth Workshop on Algorithm Engineering and Experiments (ALENEX)*, pp. 28–42, SIAM, 2017.
- [15] J. Gray, “quimb: a python library for quantum information and many-body calculations,” *Journal of Open Source Software*, vol. 3, no. 29, p. 819, 2018.
- [16] C. Huang, F. Zhang, M. Newman, J. Cai, X. Gao, Z. Tian, J. Wu, H. Xu, H. Yu, B. Yuan, *et al.*, “Classical simulation of quantum supremacy circuits,” *arXiv preprint arXiv:2005.06787*, 2020.
- [17] F. Li, X. Liu, Y. Liu, P. Zhao, Y. Yang, H. Shang, W. Sun, Z. Wang, E. Dong, and D. Chen, “Sw_qsim: a minimize-memory quantum simulator with high-performance on a new sunway supercomputer,” in *Proceedings of the International Conference for High Performance Computing, Networking, Storage and Analysis*, pp. 1–13, 2021.
- [18] H. Fu, J. Liao, J. Yang, L. Wang, Z. Song, X. Huang, C. Yang, W. Xue, F. Liu, F. Qiao, *et al.*, “The sunway taihulight supercomputer: system and applications,” *Science China Information Sciences*, vol. 59, no. 7, pp. 1–16, 2016.
- [19] S. Williams, A. Waterman, and D. Patterson, “Roofline: An insightful visual performance model for floating-point programs and multicore architectures,” 9 2009.
- [20] G. Evenbly and G. Vidal, “Tensor network renormalization,” *Physical review letters*, vol. 115, no. 18, p. 180405, 2015.
- [21] A. Cichocki, A.-H. Phan, Q. Zhao, N. Lee, I. V. Oseledets, M. Sugiyama, and D. Mandic, “Tensor networks for dimensionality reduction and large-scale optimizations. part 2 applications and future perspectives,” *arXiv preprint arXiv:1708.09165*, 2017.
- [22] M. A. Porter, J.-P. Onnela, P. J. Mucha, *et al.*, “Communities in networks,” *Notices of the AMS*, vol. 56, no. 9, pp. 1082–1097, 2009.